Wide-Bandwidth, Tunable, Multiple-Pulse-Width Optical Delays Using Slow Light in Cesium Vapor

Ryan M. Camacho, Michael V. Pack, and John C. Howell

Department of Physics and Astronomy, University of Rochester, Rochester, New York 14627, USA

Aaron Schweinsberg and Robert W. Boyd

Institute of Optics, University of Rochester, Rochester, New York 14627, USA
(Received 13 September 2006; published 10 April 2007)

We demonstrate an all-optical delay line in hot cesium vapor that tunably delays 275 ps input pulses up to 6.8 ns and 740 input ps pulses up to 59 ns (group index of approximately 200) with little pulse distortion. The delay is made tunable with a fast reconfiguration time (hundreds of ns) by optically pumping out of the atomic ground states.

There is considerable practical interest in developing all-optical delay lines that can tunably delay short pulses by much longer than the pulse duration. Slow light (i.e., the passage of light pulses through media with a small group velocity) has long been considered a possible mechanism for constructing such a delay line. Most commonly, the steep linear dispersion associated with a single gain or transparency resonance provides the group delay. Most early work used the dispersion associated with electro-magnetically induced transparency [1–7], but recently other resonances have been explored, including coherent population oscillations [8–10], stimulated Brillouin scattering [11–14], stimulated Raman scattering [15,16], and spectral hole burning [17].

In addition to single-resonance systems, double gain resonances have been used for pulse advancement [18–23] and delay [24]. Widely spaced gain peaks create a region of anomalous dispersion, resulting in pulse advancement. When the spacing between the gain peaks is small, a region of normal dispersion is created, resulting in pulse delay. Pulse advancement is also possible by the proper spacing of two absorbing resonances [22]. The possibility of pulse delay between two absorbing resonances has also received some attention [25–30].

Ideally, an optical delay line would delay high-bandwidth pulses by many pulse lengths in a short propagation distance without introducing appreciable pulse distortion and be able to tune the delay continuously with a fast reconfiguration rate. Minimal pulse absorption is also desirable, but not necessary because absorption can be compensated through amplification. Relatively few experiments [1,4,7,11,17,28] have directly measured pulse delays longer than the incident pulse duration, and of these, none has used pulses shorter than 2 ns or reported reconfiguration rates approaching the inverse pulse delay time.

In this Letter, we demonstrate the tunable delay of a 1.6-GHz-bandwidth pulse by up to 25 pulse widths and the tunable delay of a 600-MHz-bandwidth pulse by up to 80 pulse widths by making use of a double absorption reso-

nance in cesium. Furthermore, we show that the delay can be tuned with a reconfiguration time of hundreds of nanoseconds.

In a medium with two Lorentzian absorption resonances, as illustrated in Fig. 1, the complex index of refraction can be approximated as

$$n(\delta) = 1 - \frac{\mathcal{A}}{2}\left(\frac{g_1}{\delta + \Delta_+ + i\gamma} + \frac{g_2}{\delta - \Delta_- + i\gamma}\right), \quad (1)$$

where 2γ is the homogeneous linewidth [full width at half maximum (FWHM)], g_1 and g_2 account for the possibility of different strengths for the two resonances, $\delta = \omega - \omega_0 - \Delta$ is the detuning from peak transmission, $\omega_0 = (\omega_1 + \omega_2)/2$, ω_1 (ω_2) is the resonance frequency for transition 1 (transition 2), $\Delta_\pm = \omega_{21} \pm \Delta$, $\omega_{21} = (\omega_2 - \omega_1)/2$, and
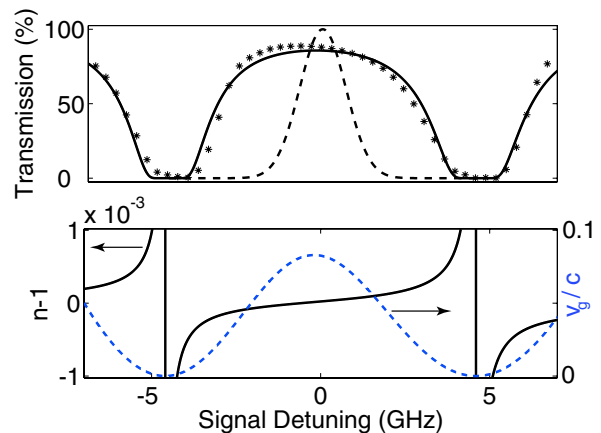

FIG. 1 (color online). (a) cw signal transmission (asterisks—measured, solid line—fit) overlaid with the spectrum (dashed line) of a 275 ps pulse and (b) index of refraction (solid line) and group velocity (dashed line), all vs signal detuning for cesium at approximately 114 °C. All theory curves taken from Eq. (1) with $\mathcal{A} = 4 \times 10^5$ rad/s, $g_1 = 7/16$, and $g_2 = 9/16$. High-fidelity optical delay is observed for light pulses passing through the nearly transparent window between the two resonances.

$$\Delta = \frac{g_1^{1/3} - g_2^{1/3}}{g_1^{1/3} + g_2^{1/3}} \omega_{21}. \qquad (2)$$

For example, alkali atoms have two hyperfine levels associated with their electronic ground state, leading to two closely spaced absorption resonances. We note that any other system with two similar absorbing resonances may also be used (e.g., quantum dots, microresonators, photonic crystals, etc.). For a vapor of alkali atoms, the detunings satisfy $\Delta_+ \approx \Delta_- \gg \gamma$, and the strength of the resonance is given in SI units by $\mathcal{A} = N|\mu|^2/[\epsilon_0\hbar(g_1 + g_2)]$, where μ is the effective far-detuned dipole moment [31], and g_1 and g_2 are proportional to the degeneracies of the hyperfine levels.

Equation (1) is also applicable for inhomogeneously broadened lines, such as Doppler broadened atomic vapors, if the detunings Δ_- and Δ_+ are greater than the inhomogeneous linewidth by an order of magnitude or more. This result holds because the homogenous Lorentzian line shape has long wings while the inhomogeneous line shape decreases exponentially.

By expanding Eq. (1) about the point $\delta = 0$, we find that the real part n' and imaginary part n'' of the index of refraction are given by

$$n'(\delta) \approx 1 + K_0 + K_1 \frac{\mathcal{A}}{\omega_{21}^2}\delta + K_3 \frac{\mathcal{A}}{\omega_{21}^4}\delta^3 \qquad (3a)$$

$$n''(\delta) \approx K_1 \frac{\mathcal{A}\gamma}{\omega_{21}^2} + 3K_3 \frac{\mathcal{A}\gamma}{\omega_{21}^4}\delta^2, \qquad (3b)$$

where

$$K_i = \left(\frac{g_1^{1/3} + g_2^{1/3}}{2}\right)^{i+1} [g_1^{(2-i)/3} + (-1)^{i+1} g_2^{(2-i)/3}], \qquad (4)$$

and where we have assumed that $n - 1 \ll 1$ in keeping only the first few terms in the expansion. Note that for the special case in which the two resonances are of equal strength (i.e., $g_1 = g_2 = g$), the coefficients are given by $K_i = 2g$ for i odd and $K_i = 0$ for i even. For cesium, which has $g_1 = 7/16$ and $g_2 = 9/16$, the error introduced by assuming $g_1 = g_2$ is approximately 0.5%. For this reason, we make the simplifying assumption $g_1 = g_2 = 1/2$ throughout the remainder of the Letter.

Pulse propagation can be described in terms of various orders of dispersion, which can be determined through use of Eq. (3a) as

$$\beta_j = \frac{1}{c} \frac{d^j \omega n'(\omega)}{d\omega^j}\bigg|_{\omega = \omega_0 + \Delta}. \qquad (5)$$

Thus the group velocity is given by $v_g = 1/\beta_1$, and the group-velocity dispersion (GVD) and third-order-dispersion are given, respectively, by β_2 and β_3. The absence of second-order (first-order) frequency dependence in Eq. (3a) and (3b) means that near $\delta = 0$ the GVD (absorption) is minimized regardless of possible differences between g_1 and g_2. Thus, between two absorption

resonances, which can be described by Eq. (1), the maximum transparency is accompanied by a minimum in GVD.

We next develop a simple model to provide an understanding of the role of dispersion and absorption on pulse broadening. We provisionally define the pulse width as the square root of the variance of the temporal pulse shape. For an unchirped Gaussian pulse, i.e., $E(0, t) = E_0 \exp(-t^2/2T_0^2)$, the pulse width defined in this way is simply T_0. The pulse width after propagating through a distance L of dispersive medium is then given to third order in δ by [32]

$$T_d^2 = T_0^2 + \left(\frac{2\beta_2 L}{T_0}\right)^2 + \left(\frac{\beta_3 L}{2T_0^2}\right)^2, \qquad (6)$$

where T_0 is the initial pulse width. In the case of cesium, where $\omega_0 \approx 2\pi \times 3.5 \times 10^{14}$ rad/s and $\omega_{21} \approx \pi \times 9.2 \times 10^9$ rad/s, β_2 can be neglected and Eq. (6) simplifies to

$$T_d^2 \approx T_0^2 + \left(\frac{3\tau_d}{\omega_{21}^2 T_0^2}\right)^2, \qquad (7)$$

where β_3 has been calculated using Eqs. (5) and (3) and where $\tau_d \approx \alpha_0 L/2\gamma$ is the pulse delay and $\alpha_0 L = 2\omega_0 n'' L/c$ is the optical depth at the pulse carrier frequency ω_0. We further note that the change in pulse width due to absorption only can be approximated as [28,33]

$$T_a^2 = T_0^2 + \frac{6\gamma\tau_d}{\omega_{21}^2}, \qquad (8)$$

so long as $(T_a/T_0 - 1) < 1$.

The fractional broadening due to dispersion, defined as $T_d/T_0 - 1$, scales as $1/T_0^3$, while the broadening due to absorption scales as $1/T_0$. In the present study, $\tau_d \approx 10^{-8}$ s, $\omega_{21} \approx 10^{11}$ rad/s, $T_0 \approx 10^{-10}$ s, and $\gamma \approx 10^7$ rad/s, indicating that dispersion is the dominant form of broadening by about 3 orders of magnitude, and the absorptive contribution to broadening can be ignored.

Experimentally it is much easier to quantify pulse widths in terms of their FWHM rather than in terms of their variance as we have done in Eqs. (6)–(8). In the remainder of this Letter, we will quote pulse widths in terms of their FWHM.

Our experimental setup is shown in Fig. 2. The signal laser is a cw diode laser with a wavelength of 852 nm. The signal frequency is tuned to obtain maximum transmission between the two Cs D_2 hyperfine resonances and is pulsed at a pulse repetition frequency of 100 kHz using a fast electro-optic modulator (EOM). The signal beam is collimated to a diameter of 3 mm, and two different pulse widths are used, 275 ps or 740 ps FWHM, with a peak intensity of less than 10 mW/cm². The pulses then pass through a heated 10-cm-long glass cell containing atomic cesium vapor. The 275 ps pulses are measured using a 7.5 GHz silicon photodiode, and the 740 ps pulses are measured with a 1 GHz avalanche photodiode. All electrical signals are recorded with a 30 GHz sampling oscillo-
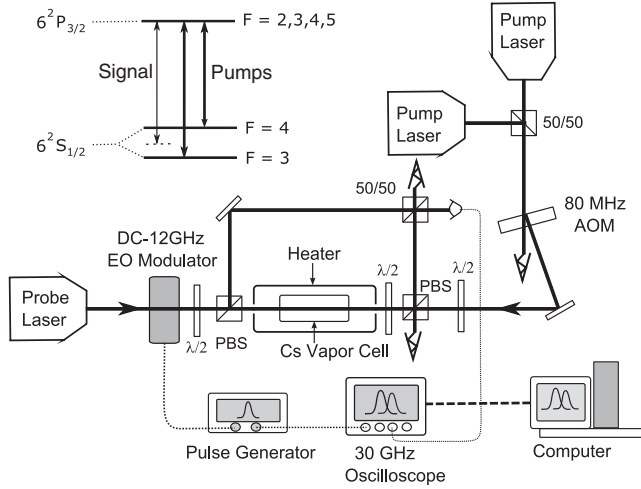
FIG. 2.   Experimental schematic. A signal pulse passes through a heated cesium vapor cell. Two pump beams combine on a beam splitter and counterpropagate relative to the signal beam through the vapor to provide tunable delay of the signal pulse.

scope triggered by the pulse generator. The pump beams are turned off except for the experiments reported in Figs. 5 and 6.

Figure 1(a) shows the transmission of a cw optical beam as a function of frequency near the two cesium hyperfine resonances, overlaid with the spectrum of a 275 ps Gaussian pulse. The data points are measured values and the solid line fits these points to the imaginary part of Eq. (1). The entire pulse spectrum lies well within the relatively flat transmission window between the resonances, resulting in little pulse distortion from absorption. Figure 1(b) shows the index of refraction [real part of Eq. (1)] and frequency-dependent group velocity associated with the absorption shown in Fig. 1(a). We note that, in the region of the pulse spectrum, the curvature of the
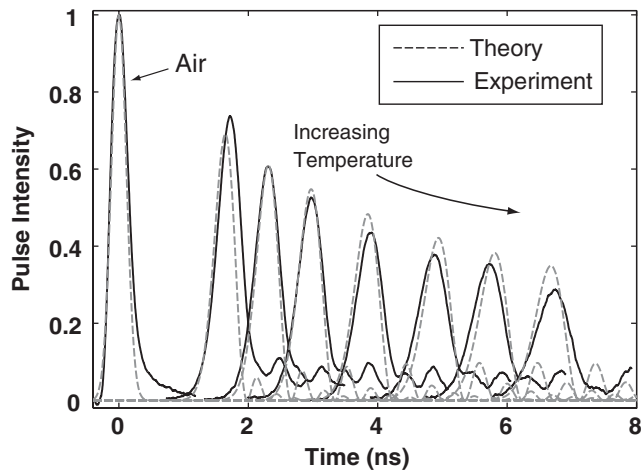
frequency-dependent group velocity is greater than that of the absorption, suggesting that dispersion is the dominant form of pulse distortion. This is not the case for single-Lorentzian systems, where the spectral variation of absorption is the dominant form of distortion [34]. While most slow light experiments have worked by making highly dispersive regions transparent, we have worked where a highly transparent region is dispersive.

As shown above, the delay of a pulse is proportional to the optical depth of the vapor. Figure 3 shows that we can control the delay by changing the temperature (and thus optical depth) of the Cs cell. Using a 10 cm cell, and varying the temperature between approximately 90 °C and 120 °C, we were able to tune the delay of a 275 ps pulse between 1.8 ns and 6.8 ns. The theory curves in Fig. 3 were obtained using $I(x, t) = n'(0)c\epsilon_0|E(z, t)|^2/2$, where the electric field is given by

$$E(z, t) = \frac{E_0 T_0 \exp[-i(\omega_0 + \Delta)t]}{\sqrt{2\pi}}$$

$$\times \int_{-\infty}^{\infty} d\delta \exp\left[i\left(\frac{\omega n(\delta)}{c}z - \delta t\right) - \frac{\delta^2 T_0^2}{2}\right], \quad (9)$$

and where we have used Eq. (1) for the index of refraction. The atomic density N has been chosen separately to fit each measured pulse. We note that a pulse may be delayed by many pulse widths relative to free-space propagation with little broadening.

Longer pulses lead to delay with reduced pulse broadening because pulse broadening is approximately proportional to $1/T_0^3$ [see Eq. (7)]. To study the larger fractional delays enabled by this effect, we used longer 740 ps input pulses for which the dispersive broadening is significantly reduced. Figures 4(a) and 4(b) show the delay and broadening of a 740 ps pulse after passing through a sequence of three 10 cm cesium vapor cells. The plots correspond to a temperature range of approximately 110 °C to 160 °C.

FIG. 3.   Pulse shapes of 275 ps input pulses transmitted through a cesium vapor cell. Delays a large as 25 pulse widths are observed. The temperature range from 90 °C to 120 °C.
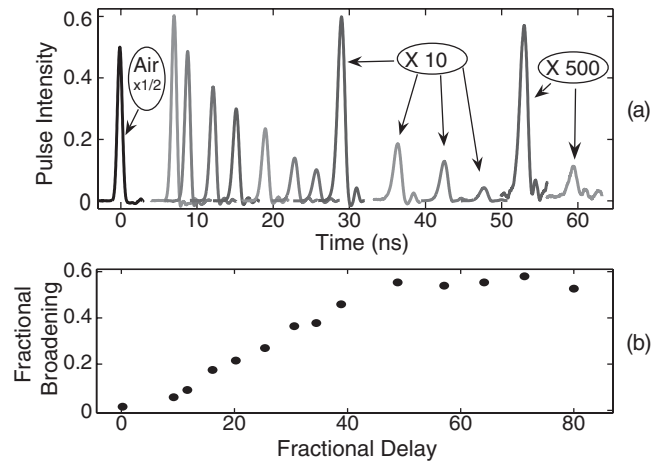

FIG. 4.   (a) Output pulse shapes and (b) fractional broadening as functions of fractional delay for a 740 ps input pulse. Fractional delay is defined as (τ_d/T_0) and fractional broadening is defined as $(T - T_0)/T_0$.
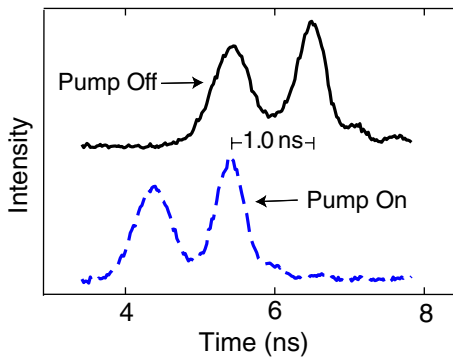
FIG. 5 (color online). Pulse output waveforms with auxiliary pump beams on (dotted line) and off (solid line). Two 275 ps input pulses separated by 1 ns are delayed by approximately 5.3 ns without pumping, but only 4.3 ns with pumping (a change of 1 bit slot) with little change in pulse shape.

Even though the pulse experiences strong absorption at large delays, the fractional broadening of the pulse FWHM remains relatively low.

In addition to temperature tuning, the optical depth can be changed much more rapidly by optically pumping the atoms into the excited state using two pump lasers. As shown in Fig. 2 each pump laser is resonant with one of the D_2 transitions in order to saturate the atoms without optical pumping from one hyperfine level to the other. The power of each pump beam is approximately 30 mW, and both pump beams are focused at the cell center. The signal beam overlaps the pump beams and is also focused to a 100 μm beam diameter. The pump beams are turned on and off using an 80 MHz acousto-optic modulator with a 100 ns rise or fall time. Being on resonance with the D_2 transitions, the pump fields experience significant absorption ($\alpha L \sim 300$), and are entirely absorbed despite having intensities well above the saturation intensity.

With the pump beams on, the decreases in effective ground-state atomic density leads to smaller delay. Figure 5 shows a delayed pulse waveform consisting of two 275 ps input pulses separated by 1 ns, with the pump on and off. We note that pump fields create no noticeable change in the waveform shape or amplitude. Also, we measured that the change in delay is essentially proportional to the pump power.

In Fig. 6 the measured signal delay is shown as a function of the difference between arrival time t_s of the signal at the cell and the turn-on time t_p of the pump. The rise and fall times lie in the range 300–600 ns and vary slightly depending on the relative detunings of the pumps.

In summary, we have observed large tunable fractional time delays of high-bandwidth pulses with fast reconfiguration rates and low distortion by tuning the laser frequency between the two ground-state hyperfine resonances of a hot atomic cesium vapor cell. We have shown that in such a medium, dispersion is the dominant form of broadening, and we have characterized the delay, broadening, and reconfiguration rates of the delayed pulses.
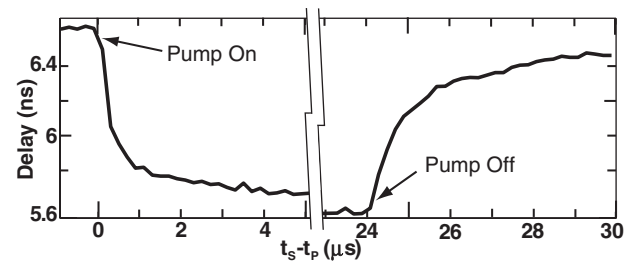

FIG. 6. Pulse delay vs time following pump turn-on and turn-off, showing the reconfiguration time for optically tuning the pulse delay. The two pump beams are tuned to separate cesium hyperfine resonances and are switched on at the time origin and switched off 24 μs later.

[1] A. Kasapi *et al.*, Phys. Rev. Lett. **74**, 2447 (1995).
[2] M. M. Kash *et al.*, Phys. Rev. Lett. **82**, 5229 (1999).
[3] D. Budker *et al.*, Phys. Rev. Lett. **83**, 1767 (1999).
[4] L. V. Hau *et al.*, Nature (London) **397**, 594 (1999).
[5] D. F. Phillips *et al.*, Phys. Rev. Lett. **86**, 783 (2001).
[6] C. Liu *et al.*, Nature (London) **409**, 490 (2001).
[7] A. Turukhin *et al.*, Phys. Rev. Lett. **88**, 023602 (2001).
[8] M. S. Bigelow *et al.*, Science **301**, 200 (2003).
[9] X. Zhao *et al.*, Opt. Express **13**, 7899 (2005).
[10] P. Palinginis *et al.*, Opt. Express **13**, 9909 (2005).
[11] K. Y. Song *et al.*, Opt. Lett. **30**, 1782 (2005).
[12] Y. Okawachi *et al.*, Phys. Rev. Lett. **94**, 153902 (2005).
[13] M. Gonzalez-Herraez *et al.*, Appl. Phys. Lett. **87**, 081113 (2005).
[14] M. Gonzalez-Herraez *et al.*, Opt. Express **14**, 1395 (2006).
[15] J. E. Sharping *et al.*, Opt. Express **13**, 6092 (2005).
[16] D. Dahan *et al.*, Opt. Express **13**, 6234 (2005).
[17] R. M. Camacho *et al.*, Phys. Rev. A **74**, 033801 (2006).
[18] R. Y. Chiao, Phys. Rev. A **48**, R34 (1993).
[19] L. J. Wang *et al.*, Nature (London) **406**, 277 (2000).
[20] A. Dogariu *et al.*, Phys. Rev. A **63**, 053806 (2001).
[21] M. D. Stenner *et al.*, Nature (London) **425**, 695 (2003).
[22] B. Macke *et al.*, Eur. Phys. J. D **23**, 125 (2003).
[23] G. S. Agarwal *et al.*, Phys. Rev. A **70**, 023802 (2004).
[24] M. D. Stenner *et al.*, Opt. Express **13**, 9995 (2005).
[25] D. Grischkowsky, Phys. Rev. A **7**, 2096 (1973).
[26] H. Tanaka *et al.*, Phys. Rev. A **68**, 053801 (2003).
[27] B. Macke *et al.*, Phys. Rev. A **73**, 043802 (2006).
[28] R. M. Camacho *et al.*, Phys. Rev. A **73**, 063812 (2006).
[29] Z. Zhu *et al.*, Opt. Express **14**, 7238 (2006).
[30] R. M. Camacho *et al.*, Phys. Rev. Lett. **98**, 043902 (2007).
[31] D. A. Steck, Los Alamos National Laboratory Technical Report No. LA-UR-03-7943, 2003; http://steck.us/alkalidata/.
[32] G. P. Agrawal, *Nonlinear Fiber Optics* (Academic, New York, 1995), p. 79.
[33] R. W. Boyd *et al.*, Phys. Rev. A **71**, 023801 (2005).
[34] R. W. Boyd *et al.*, *Progress in Optics* (Elsevier, New York, 2002), p. 497.